

Catalytic properties of a CuO–CeO₂ sorbent-catalyst for de-SO_x reaction

Arturo Rodas-Grapaín^{a,b}, Jesús Arenas-Alatorre^a,
Antonio Gómez-Cortés^a, Gabriela Díaz^{a,*}

^a Instituto de Física, UNAM, P.O. Box 20-364, C.P. 01000, México, D.F., Mexico

^b IIE, Reforma 113, Colonia Palmira, Cuernavaca, Morelos 62490, Mexico

Available online 24 August 2005

Abstract

The preparation and characterization of a CuO–CeO₂ sorbent-catalyst was performed by an inorganic/organic synthesis route and the materials were tested in de-SO_x type reactions. The preparation of mesostructured CeO₂ was made using hexadecylamine surfactant and cerium acetate as the inorganic precursor. This procedure was modified by inclusion of the CuO precursor during the synthesis. These sorbent-catalysts were characterized by transmission electronic microscopy (TEM), N₂ physisorption, X-ray diffraction (XRD) and temperature-programmed reduction (TPR). The adsorbent-catalysts were tested by means of sulfurization from room temperature to 760 °C using a combined SO₂/N₂ gas mixture (3600 ppm) and the gain of weight was recorded in a thermo-balance. The materials prepared with those surfactants showed high surface area due to mesopores and small CuO particles dispersed on the ceria support. The catalytic performance in the de-SO_x reaction was higher than conventional sorbent-catalysts prepared by impregnation of commercial ceria. The improved SO₂ adsorption capacity of these materials is attributed to a better distribution and interaction of the copper species with the ceria support.

© 2005 Elsevier B.V. All rights reserved.

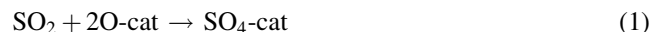
Keywords: de-SO_x; Ceria; Copper oxide; Flue gas desulfurization; Sulfur dioxide; Surfactants

1. Introduction

One of the main sources of sulfur dioxide (SO₂) is the combustion of fossil fuels in electric power generation plants. This hazardous gas is highly corrosive and toxic at moderate concentrations in air and it is a known precursor of acid rain. Several technologies have been developed for de-SO_x (SO₂, SO₃) and emission control known as flue gas desulfurization (FGD) technologies. Some of these technologies are based in catalytic processes, which use potassium oxide on vanadia (V₂O₅) or copper oxide (CuO) on alumina (γ-Al₂O₃) as sorbent-catalysts.

Second generation de-SO_x catalysts have been applied to flue gas desulfurization, for example, those based on cerium dioxide CeO₂ [1]. This oxide has a high oxygen storage capacity (OSC) due to its redox properties, which are

associated to the easy change between Ce⁴⁺/Ce³⁺ oxidation states. Ceria (cerium dioxide) has been used as support in different chemical process such as wastewater treatment, fuel cells, three-way catalyst (TWC) for NO_x reduction in automobile exhaust gas emissions, catalytic hydrocarbon combustion, flue gas desulfurization (FGD) at high temperature, the gasification of fossil fuels, as well as other processes [1–6]. The surface oxygen availability in ceria can be applied in the flue gas desulfurization of thermoelectric power plants, i.e., the oxidation of the sulfur dioxide present in exhaust gases. The de-SO_x reaction that is carried out with this kind of sorbent-catalysts is the following [7]:



This process can be efficiently carried out at high temperatures (>500 °C) and the sulfate adsorbed on the surface can be reduced by methane (natural gas), carbon monoxide, ammonia or hydrogen.

* Corresponding author. Tel.: +52 55 56225097; fax: +52 55 56225008.
E-mail address: diaz@fisica.unam.mx (G. Díaz).

On the other hand, conventional ceria has poor textural properties in general, such as low surface area, but those properties could be improved if the preparation procedure is modified or a promoter is added [4]. Synthesis methods reported in the literature that increases the surface area and produce meso-structured materials is related to the use of surfactants as liquid crystal templating (LCT) agents to create a regular three-dimensional micelles array about which an inorganic precursor could form a framework. Several works have been reported concerning the preparation of mesoporous ceria by this method using ionic or neutral templates, cerium(III) chloride, CeCl_3 , and cerium(III) acetate, $\text{Ce}(\text{C}_2\text{H}_3\text{O}_2)_3$ as ceria inorganic precursors [8–10]. On the other hand, combining the ceria with transition metals using the classic impregnation methods improves the oxygen storage capacity (OSC) [11–13].

In this work, the preparation, characterization and performance of sorbent-catalysts based on copper oxide, CuO, and CeO_2 are described. The material was prepared using the LCT method based in a procedure reported by Lyons et al. [10] for meso-structured CeO_2 . This procedure was modified by including the CuO precursor during the synthesis of cerium oxide. The material was characterized by means of several techniques such as TEM, nitrogen adsorption (surface area and pore size distribution), X-ray diffraction (XRD) and temperature-programmed reduction (TPR). The catalytic properties of these materials for de- SO_x reactions were studied under various experimental conditions by thermogravimetric analysis (TGA). The performance of the materials was compared to other materials prepared by conventional methods.

2. Experimental

2.1. Catalyst preparation

In a first step CeO_2 was prepared according to the literature following the procedure described by Lyons et al. [10]. Briefly, hexadecylamine (Aldrich, $\text{C}_{16}\text{H}_{35}\text{N}$) was added to a 50% aqueous ethanol solution under stirring for several minutes. A molar ratio of inorganic precursor/surfactant equal to 2 was achieved by adding the required quantity of cerium precursor, i.e., hydrated cerium(III) acetate (Aldrich, $\text{Ce}(\text{C}_2\text{H}_3\text{O}_2)_3 \cdot x\text{H}_2\text{O}$). This mixture was stirred for 1 h at room temperature then placed in an oven at 60 °C for 48 h. The precipitate formed was washed with ethanol–water mixtures, then filtered out and washed again with de-ionized water. The resultant solids were submitted to various thermal treatments; first at 128 °C for 6 h then were calcined under extra-dry air at 285 °C for 4 h. The products show a pale-yellow color, which is characteristic of hydrated cerium di-oxide powder [14]. For the CuO– CeO_2 samples the preparation procedure was about the same as before with an additional step, that is the incorporation of the copper precursor (hydrated copper nitrate, $\text{Cu}(\text{NO}_3)_2 \cdot 3\text{H}_2\text{O}$, Fluka)

once the precipitated was formed. This mixture was stirred for 10 more minutes at room temperature and then it was placed in an oven at 60 °C for 48 h. The precipitate was filtered without further washing steps. The samples were submitted to the same thermal treatments previously described, then dried at 128 °C for 6 h and calcined at 285 °C for 4 h. The nominal copper loading was 1 and 4 wt.%. These calcined materials showed an olive-green color.

On the other hand, the reference catalysts were those obtained by classical impregnation, i.e., CuO/ CeO_2 prepared from supports based on commercial ceria (Aldrich) and the home made CeO_2 . In this case the support was impregnated with hydrated copper(II) nitrate solution to get a nominal copper loading around 1 and 5 wt.%. All these materials were dried in an oven at 90 °C for 12 h and calcined in extra-dry air at 350 °C for 3 h. The actual copper content was determined by atomic absorption spectrometry. Hereafter the samples are identified as follows: CeO_2M stands for the ceria synthesized in this work, CuCeM refers to copper containing samples in which the copper precursor was incorporated during the synthesis of the support; CuCeI and CuCe O_2M refer to samples prepared by classical impregnation of the copper precursor on the surface of a commercial ceria (CuCeI) or using the CeO_2M support (CuCe O_2M), respectively. A and B refers to low or high copper loading, respectively.

2.2. Catalyst characterization

The microstructural characterization of the materials prepared from templating agents was performed in a JEOL 2010 FASTEM microscope. The textural properties such as specific surface area, pore volume and pore size distribution were determined using a Quantachrome Autosorb system with nitrogen gas as adsorbate. The crystalline structure of the solids was studied by X-ray diffraction (XRD) using a Brucker D-8 diffractometer equipped with a Cu $\text{K}\alpha$ radiation source and from $2\theta = 0.05$ to 80 with a 0.04° step size. The behavior of the sorbent-catalysts in the presence of a reductive atmosphere (TPR) was studied in a multi-task unit RIG-100, using 5% H_2/He gas mixture (30 cm^3/min). All TPR tests were carried out using 50 mg samples with a heating ramp of 10 °C/min, from room temperature to 400 °C. Before the experiment the sample was submitted to nitrogen gas (80 cm^3/min) at 100 °C for 30 min to eliminate the moisture.

In order to evaluate the performance of the sorbent-catalysts for de- SO_x type reactions, several sulfurization tests were carried out at the laboratory scale, using a TA Instruments 2050 thermobalance as the reactor. The experimental set up is shown in Fig. 1. The sample (20 mg) was loaded on a platinum pan and heated at 100 °C for 30 min under nitrogen atmosphere. Afterwards the sample is flowed with 3600 ppm of SO_2/N_2 gas mixture (90 cm^3/min) at a heating ramp of 20 °C/min in the range RT–760 °C. The sulfurization tests were carried out in the

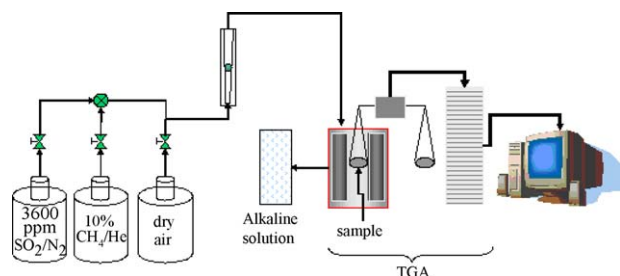


Fig. 1. Experimental set-up for sulfurization runs.

absence of the CuO-CeO_2 materials to evaluate the contribution, if any, of the platinum holder.

In addition, the sulfurization reaction at isothermal conditions (200, 300, 400 and 500 °C) was also evaluated. From an industrial point of view, the regeneration cycles are important for the FGD technologies that are applied to the thermoelectrical power plants, therefore, a series of cycles including thermal treatments in 10 vol.% CH_4/He (reduction) and extra-dry air (oxidation) flow were simulated in this work.

3. Results and discussion

3.1. Characterization

All the samples prepared by the LCT method (CeO_2M and CuCeM) showed similar morphological features by HRTEM. Fig. 2 shows a typical TEM image of the CuCeMA sorbent-catalysts dried and pre-calcined at 128 °C for 6 h. This figure clearly shows the typical mesoporous order in the inner structure of the materials, showing that the addition of the copper precursor during the preparation did not affect the CeO_2 structure. When this material is calcined at 285 °C for 4 h the ordered structure is lost and a worm-like structure was observed (Fig. 3) and long range mesoporous order was not observed even after the calcination process at high temperature.

Despite the loss of the long-range mesoporous order the relative surface area of these sorbent-catalysts is high ($\sim 160 \text{ m}^2/\text{g}$), as shown in Table 1. In comparison, the

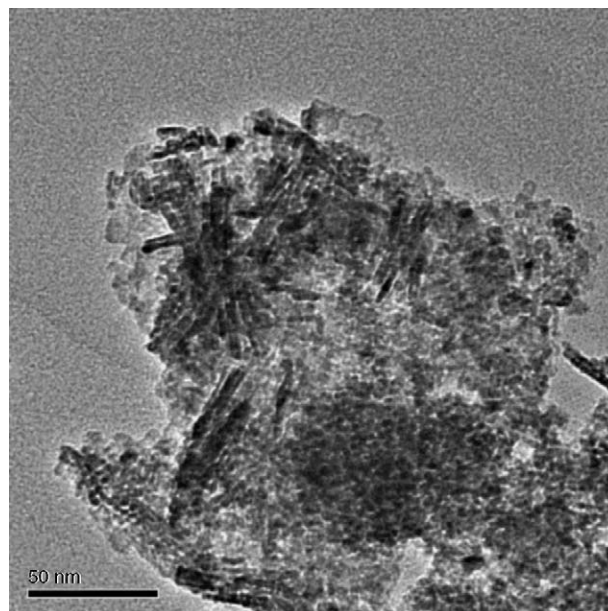


Fig. 3. TEM typical image of CuCeMA sorbent-catalyst and calcined at 285 °C for 3 h. Worm-like structure was observed.

Table 1

Specific area and actual copper content in sorbent-catalysts prepared by organic/inorganic route (surfactants) and by classic impregnation method

Sample	S_{BET} (m^2/g)	Copper loading ^a (wt.%)
CeO_2M	153.0	—
CuCeMA	163.6	1.3
CuCeMB	164.7	4.4
CuCeIA	25.3	1.5
CuCeIB	18.5	5.7

CeO_2M , CuCeMA and CuCeMB samples prepared using hexadecylamine as surfactant, CuCeIA and CuCeIB sample prepared by impregnation of a commercial CeO_2 (Aldrich).

^a Determined by atomic absorption spectroscopy.

surface area of the samples prepared using a commercial ceria is quite low ($\sim 25 \text{ m}^2/\text{g}$).

Fig. 4 shows textural features of samples prepared by LCT method. Fig. 4a shows the N_2 adsorption/desorption isotherm (type IV), which is typical for these solids as well as for mesostructured materials in general. The pore size

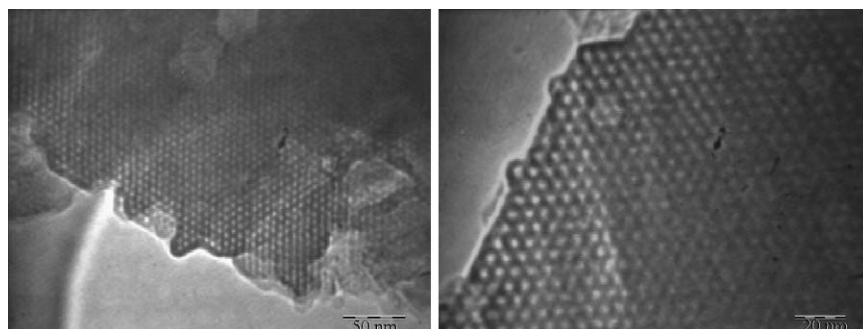


Fig. 2. TEM typical images of CuCeMA sample pre-calcined at 128 °C for 5 h. Long-order mesoporous array was observed.

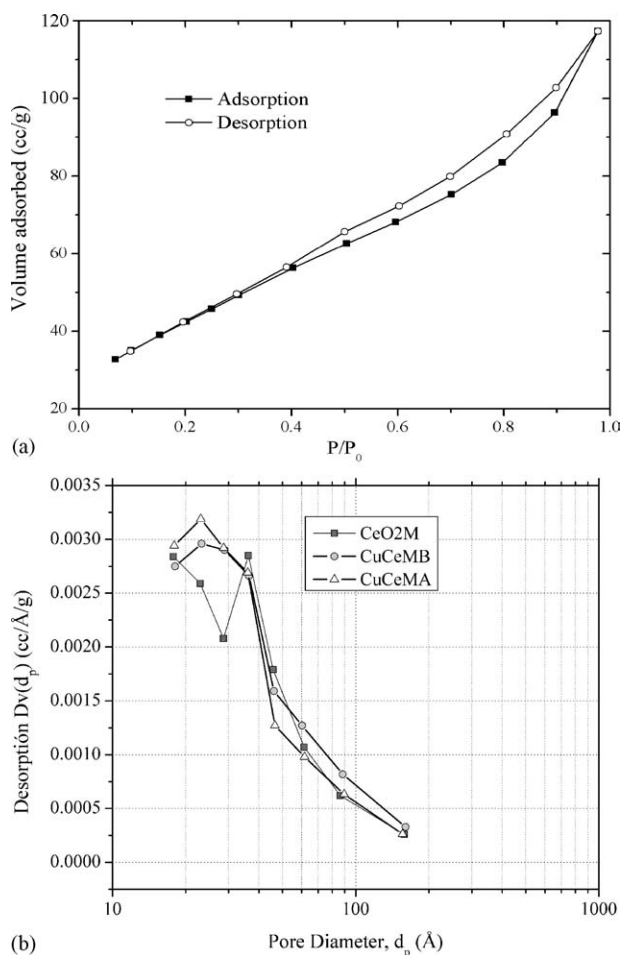


Fig. 4. Textural features of sorbent-catalysts prepared by LCT route. (a) Typical N₂ adsorption/desorption isotherm obtained for these samples, (b) pore size distribution in CuCeMA (1.3 wt.% Cu), CuCeMB (4.4 wt.% Cu) and CeO₂M samples.

distribution that was calculated using the BJH method is presented in Fig. 4b, which ranges from 2.5 to 5.0 nm.

The diffraction patterns of CeO₂M and CuCeMB sorbent-catalysts prepared by LCT method and those corresponding to CuCeIA and CuCeIB sorbent-catalysts prepared by classic impregnation of commercial ceria are shown in

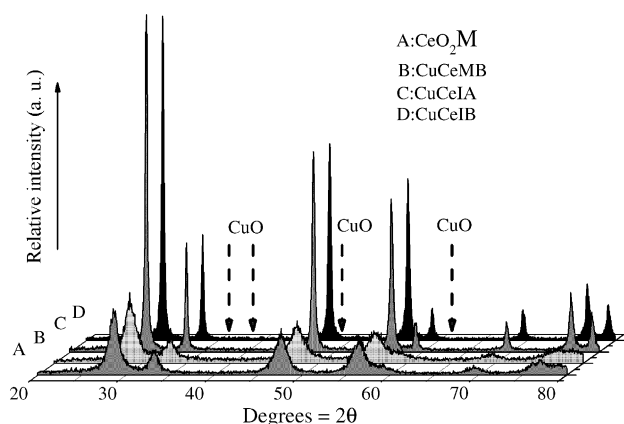


Fig. 5. X-ray diffraction patterns for (A) CeO₂M and (B) CuCeMB (4.4 wt.% Cu) and (C) CuCeIA (1.5 wt.% Cu) and (D) CuCeIB (5.7 wt.% Cu). Vertical dash line indicates the position where the most intense diffraction peaks for CuO phase should appear.

Fig. 5. The diffraction lines corresponding to the CeO₂ phase are observed in all diffraction patterns and some differences related to the intensity and shape of the main diffraction lines are evident when comparing the commercial CeO₂ with the samples prepared using the LCT method. Small broad peaks are observed for CeO₂M and CuCeMB solids (A and B patterns) while intense and well-defined diffraction peaks are observed for CuCeIA and CeCeIB samples (C and D patterns). This feature is clearly related to the crystallite size of the CeO₂ particles; LCT prepared samples are characterized by small CeO₂ nanocrystals. On the other hand, a common feature in all the diffractograms is that diffraction lines corresponding to the CuO phase are not observed. This result suggests that copper oxide crystals with a size below the resolution limit of the technique are well dispersed on the ceria support [15,16].

HRTEM characterization of the sorbent-catalysts prepared by LCT method showed the presence of small CuO and CeO₂ crystals. Fig. 6 shows the typical images of the CuCeMB sorbent-catalyst where these nanocrystals were identified (Fig. 6a and b, respectively). In addition, some other areas presented structures that were not identified as copper or cerium oxide phases. This suggests that a non-

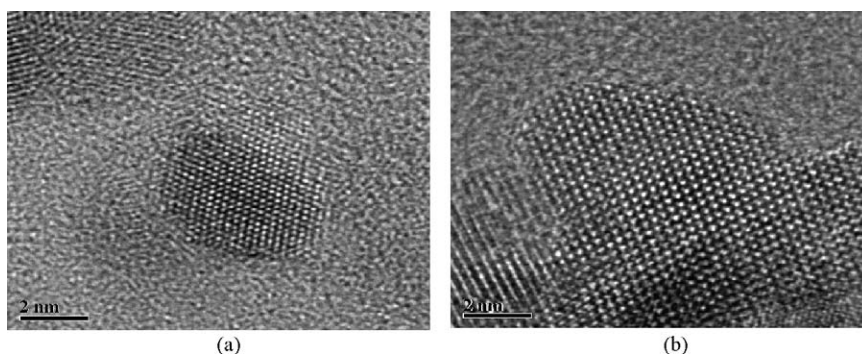


Fig. 6. HRTEM images of CuCeMB (4.4 wt.% Cu) sorbent-catalyst calcined at 285 °C for 3 h; (a) CuO and (b) CeO₂ particles.

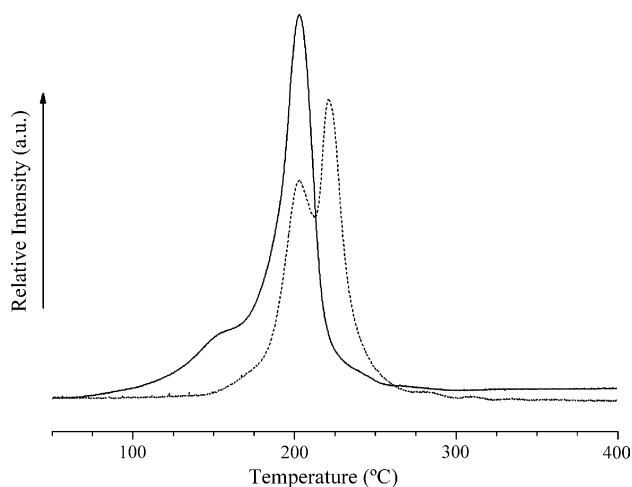


Fig. 7. TPR profiles of CuCeMA (solid line) and CuCeMB (dash line) sorbent-catalysts calcined at 285 °C for 3 h.

stoichiometric nano-structured CuCeO_x phase may also be present in these samples.

Fig. 7 shows the TPR profiles for CuCeMA (solid line) and CuCeMB (dash line) samples, respectively. TPR profiles are characterized by two hydrogen consumptions which maxima are located at different temperature. The profile for the CuCeMA material shows an intense peak with a maximum at 200 °C and a shoulder at around 150 °C. For the CuCeMB sample two contributions are observed: the first one at 180 °C and the second at 220 °C. The peaks observed in TPR profiles could be related to different kinds of copper species on the surface of the catalysts. Luo et al. [17] have reported that well dispersed copper oxide on ceria can be reduced at lower temperatures than the pure oxide. Therefore, we could assign in Fig. 7 the lower and higher reduction temperature to the reduction of small and larger CuO particles, respectively. The TPR profile showed at higher temperatures (around 500 °C) hydrogen consumption related to reduction of CeO_2 . Quantitative analysis showed, on the other hand, that the hydrogen uptake related with the peaks shown in Fig. 7 is higher compared to the theoretical value assuming complete reduction of all copper species ($\text{Cu}^{2+} \rightarrow \text{Cu}^0$) present in the sorbent-catalyst. As a confirmation of this result a TPR experiment performed using TGA (not presented) showed a 20% difference between the theoretical and the actual observed weight loss. This result may indicate that reduction of the ceria support could take place at low temperature and promoted by the presence of copper in the sorbent-catalyst. Thus, the presence of copper oxide may have some effect on the redox capacity of the CeO_2 that can improve its performance in oxidation processes [13,16,17].

3.2. SO_2 adsorption capacity

The performance of the solids for de- SO_x reactions was followed by TGA and the results are shown in Fig. 8. All the

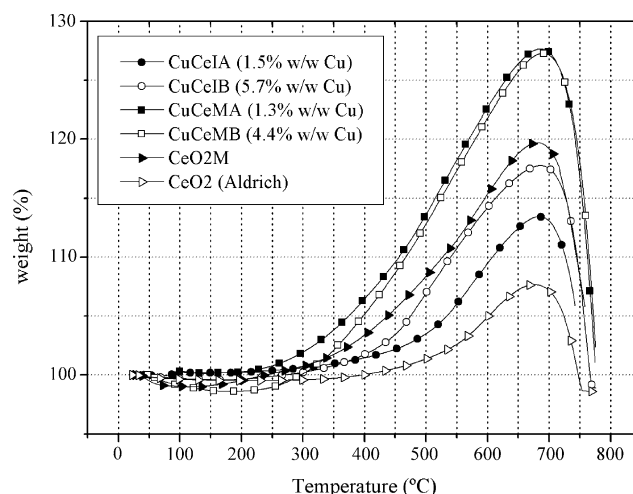


Fig. 8. Sulfurization runs as a function of temperature. Comparison of the properties of classical impregnated (commercial ceria) and prepared by surfactants sorbent-catalysts.

curves show a volcano type profile with a maximum adsorption around 700 °C, which is related to the stability of the SO_2 adsorbed on the surface [18]. As observed in Fig. 8, the adsorption capacity of the bare CeO_2 , the commercial (Aldrich) CeO_2 and the CeO_2M is different from each other. The CeO_2M oxide presents a higher adsorption capacity. According to Ferrizz et al. [18] and Zhu et al. [19], cerium dioxide can react with SO_2 over a fairly wide temperature range with or without oxygen to form adsorbed SO_2 at low temperature (room temperature) while sulfite or sulfate species form at high temperature. Thus, ceria-based sorbent-catalyst can adsorb sulfur dioxide and transform it to sulfate by an oxidation process that occurs on ceria, which in turn could be reduced to Ce^{3+} .

On the other hand, the solids series including CuO showed a higher adsorption capacity compared to the CeO_2 alone. Moreover, the sorbent-catalysts prepared by surfactants (CuCeMA and CuCeMB) present a higher performance in de- SO_x process compared to the impregnated samples. XANES studies [20] have showed that the copper presence in ceria-based sorbent-catalyst can create new active sites for sulfur dioxide adsorption on ceria. In addition to this, the high surface area present in CuCeMA and CuCeMB solids may also contribute to improve the SO_2 adsorption by this kind of materials.

On the other hand, copper loading seems not to affect the adsorption properties of these solids. The sulfurization profile and the maximum adsorption capacity is practically the same for the CuCeMA and CuCeMB samples which copper content is 1.3 and 4.3 wt.%, respectively. In the case of CuCeIA and CuCeIB sorbent-catalysts, the sample with higher copper loading (5.7 wt.%) present a better performance.

In order to examine how is the effect of incorporating copper in the CeO_2M support and how it determines its catalytic performance, Fig. 9 shows a comparison between

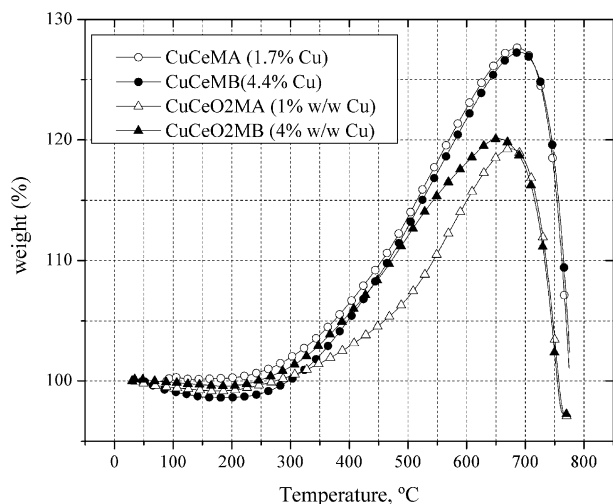


Fig. 9. Comparison of the sulfurization performance of sorbent-catalysts prepared by LCT method (CuCeM) and by classical impregnation using mesostructured CeO_2 (CuCeO₂M).

the sulfurization curves of copper oxide on ceria-based sorbent-catalysts prepared by impregnation (support CeO_2 M), home-made ceria (CuCeO₂MA, CuCeO₂MB) and the previously described CuCeMB and CuCeMA samples. As observed in Fig. 9, a better performance in the sulfurization process is observed for samples having copper incorporated during the preparation of CeO_2 (CuCeMA and CuCeMB). A possible explanation of this behavior could be linked to the LCT method, which leads to the formation of smaller CuO crystals interacting strongly with the support. An intimate relationship between the copper species and ceria could be achieved by this preparation method.

Fig. 10 shows the isothermal sulfurization at 200, 300, 400 and 500 °C using CuCeMB as sorbent-catalyst. This experiment shows that a stable sulfur species is formed on the surface of this material and that the sulfurization process depends directly on the temperature and the

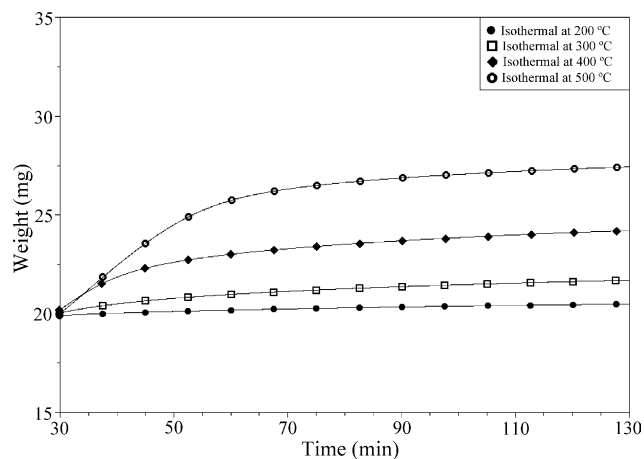


Fig. 10. Isothermal sulfurization at 200 °C (●), 300 °C (□), 400 °C (◆) and 500 °C (○) using the CuCeMB (4.4 wt.% Cu) sorbent-catalyst.

process is more efficient at higher temperatures [7,19,20].

The sulfurization tests performed with sorbent-catalysts based on $\text{CuO}/\gamma\text{-Al}_2\text{O}_3$ with similar CuO loadings [21] showed a lower adsorption capacity than copper ceria-based materials shown in Fig. 8. This difference is attributed to the oxygen storage capacity of ceria, which can improve the de- SO_x process.

Some authors have mentioned the importance of the ceria preparation method to obtain the redox sites required for de- SO_x reaction [8,22]. Therefore, the CuCeM sorbent-catalysts performance suggests that the preparation method employed (organic template) supplies more available sites for SO_2 adsorption, due to an intimate relationship between the copper species and ceria.

3.3. Regeneration (sulfuration–reduction–oxidation cycles)

From an industrial point of view, the regeneration capacity of a sorbent-catalyst is very important. In this view, the CuCeMB sorbent-catalyst was submitted to several regeneration cycles including a sequence of sulfurization (SO_2/N_2) and reduction (CH_4/He) oxidation (air) steps. For a CuCeMB sorbent-catalyst calcinated at 285 °C (not shown) a drastic drop of SO_2 adsorption capacity before the first cycle was observed. This behavior can be attributed to three possible reasons: (a) decrease of the surface area of the sorbent-catalyst during regeneration cycles; (b) CuO sintering after the first cycle due to the high reduction temperature (700 °C); (c) coke or elemental sulfur formation on the surface due to the reduction step in the presence of methane as reducing gas [7,19,23].

Fig. 11 shows, on the other hand, the behavior of CuCeMB sorbent-catalyst calcined at 700 °C for 2 h ($S_{\text{BET}} = 93.3 \text{ m}^2/\text{g}$). The drop in adsorption capacity was

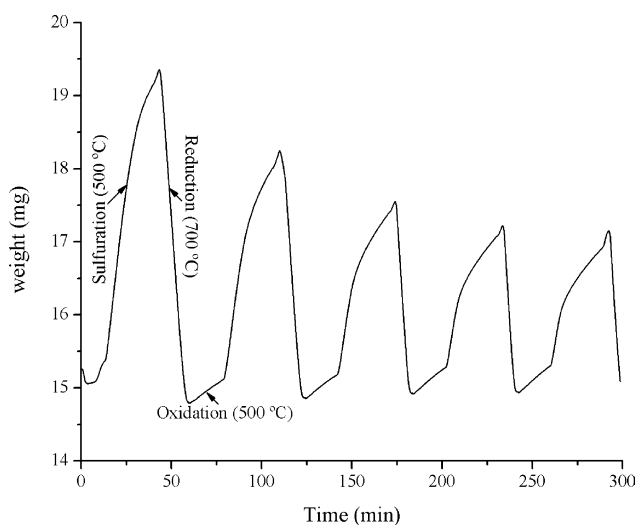


Fig. 11. Sulfuration–reduction–oxidation cycles of CuCeMB (4.4 wt.% Cu) sorbent-catalyst calcined at 700 °C for 2 h.

less than in the previous case and after the third regeneration cycle any drop of SO₂ adsorption capacity was observed although the final BET area is rather small.

4. Conclusions

CuO–CeO₂ sorbent-catalysts were prepared by an inorganic/organic LCT route. In these materials, the long range ordered mesoporous structure is lost after calcination at 285 °C, leading to a worm-like structure as evidenced by TEM and high surface area (~160 m²/g). Small CeO₂ and CuO crystallites were evidenced by HRTEM. The XRD patterns presented small and broad characteristic diffraction lines of the CeO₂ phase but any evidence of diffraction lines of the CuO phase was observed. TPR profiles of the copper species were related to reduction of small and larger CuO particles. Quantitative analysis showed, on the other hand, that a possible reduction of CeO₂ at low temperature is taking place and promoted by the presence of copper.

These materials were tested for DeSO_x reaction using 3600 ppm SO₂/N₂ gas mixture showing a better SO₂ adsorption capacity than those prepared by classical impregnation of commercial ceria. The efficiency of the process is temperature related as showed by the isothermal sulfurization experiments at 200, 300, 400 and 500 °C. The reduction process by methane of the sulfated sorbent-catalyst calcined at low temperature showed a progressive low SO₂ adsorption capacity after each regeneration cycle (sulfurization–reduction–oxidation). Several reasons may be involved, (a) loss of surface area of the sorbent-catalyst, (b) CuO sintering, and (c) coke or elemental sulfur formation during the regeneration. A sorbent-catalyst thermally stabilized at higher temperature showed a better performance for the regeneration process unless surface area is drastically lowered. The improved SO₂ adsorption capacity of the materials is attributed to a better distribution and interaction of the copper species in the ceria support due to the preparation method.

Acknowledgements

The authors would like to thank Dr. Gabriel Alonso from CIMAV for the BET measurements, Manuel Aguilar and

Pedro Huidrobo from IFUNAM for the XRD and TPR analysis, and also Georgina Blass and Guadalupe Rodríguez from IIE–Cuernavaca for the atomic absorption spectroscopy analysis.

References

- [1] Y. Zeng, S. Kaytakoglu, D.P. Harrison, *Chem. Eng. Sci.* 55 (2000) 4893.
- [2] Z. Li, M.F. Stephanopoulos, *Ind. Eng. Chem. Res.* 36 (1997) 187.
- [3] B. Wen, M. He, *Appl. Catal. B* 37 (2002) 75.
- [4] A. Trovarelli, C. de Leitenburg, M. Boaro, G. Dolcetti, *Catal. Today* 50 (1999) 353.
- [5] M. O'Connell, M.A. Morris, *Catal. Today* 59 (2000) 387.
- [6] S.W. Hedges, H.W. Pennline, *Int. J. Environ. Pollut.* 17 (1/2) (2002) 44.
- [7] W. Liu, C. Wadia, M.F. Stephanopoulos, *Catal. Today* 28 (1996) 391.
- [8] D. Terribile, A. Trovarelli, C. de Leitenburg, G. Dolcetti, J. Llorca, *Chem. Mater.* 9 (1997) 2676.
- [9] D. Terribile, A. Trovarelli, J. Llorca, C. de Leitenburg, G. Dolcetti, *J. Catal.* 178 (1998) 299.
- [10] D.M. Lyons, K.M. Ryan, M.A. Morris, *J. Mater. Chem.* 12 (2002) 1207.
- [11] J.B. Wang, S.Ch. Lin, T.J. Huang, *Appl. Catal. A: General* 232 (2002) 107–120.
- [12] M. Boaro, C. de Leitenburg, G. Dolcetti, A. Trovarelli, M. Graziani, *Topics Catal.* 16/17 (1/4) (2001) 299.
- [13] S.M. Zhang, W.D. Huang, X.H. Qiu, B.Q. Li, X.Ch. Zeng, S.H. Wu, *Catal. Lett.* 80 (2002) 41.
- [14] D.W. Green, R.H. Perry, *Perry's Chemical Engineer's Handbook*, 7th ed., New York, McGraw-Hill, 1997, pp. 2–12.
- [15] J. Xiaoyuan, L. Liping, Ch. Yingxu, Z. Xiaoming, *J. Mol. Catal. A* 197 (2003) 193.
- [16] G. Sedmak, S. Hocevar, J. Levec, *J. Catal.* 213 (2003) 135.
- [17] M.F. Luo, Y.J. Zhong, X.X. Yuan, X.M. Zheng, *Appl. Catal. A* 162 (1997) 121.
- [18] R.M. Ferrizz, R.J. Gorte, J.M. Vohs, *Catal. Lett.* 82 (1/2) (2002) 123.
- [19] T. Zhu, A. Dreher, M.F. Stephanopoulos, *Appl. Catal. B* 21 (1999) 103.
- [20] J.A. Rodríguez, T. Jirsak, A. Freitag, J.C. Hanson, J.Z. Larese, S. Chaturvedi, *Catal. Lett.* 62 (1999) 113.
- [21] A. Rodas, R. Flores, C. Palma, Y. Meléndez, X. Meléndez. *International Symposium on Advances in Hydroprocessing of Oil Fractions (ISAHOF 2004)*, Oaxaca, México, 18–22 April 2004, Paper No. 10.5.
- [22] S.H. Overbury, D.R. Mullins, D.R. Huntley, Lj. Kundakovic, *J. Phys. Chem. B* 103 (1999) 11308.
- [23] M. Flytzani-Stephanopoulos, T. Zhu, Y. Li, *Catal. Today* 62 (2000) 145.